applied sciences

MDPI

Article

Frequency Response Analysis: An Enabling Technology to Detect Internal Faults within Critical Electric Assets

Salem Mgammal Al-Ameri [1], Ahmed Allawy Alawady [2], Zulkurnain Abdul-Malek [1,*], Zulkarnain Ahmad Noorden [1], Mohd Fairouz Mohd Yousof [3,*], Ali Ahmed Salem [1], Mohamed Ibrahim Mosaad [4] and Ahmed Abu-Siada [5]

1 Institute of High Voltage and High Current, School of Electrical Engineering, Universiti Teknologi Malaysia, Johor Bahru 81310, Malaysia
2 College of Technical Engineering, The Islamic University, Najaf 54001, Iraq
3 Faculty of Electrical and Electronic Engineering, Universiti Tun Hussein Onn Malaysia, Parit Raja 86400, Malaysia
4 Electrical Engineering Department, Faculty of Engineering, Damietta University, Damietta 34511, Egypt
5 Electrical and Computer Engineering Discipline, Curtin University, Bentley, WA 6102, Australia
* Correspondence: zulkurnain@utm.my (Z.A.-M.); fairouz@uthm.edu.my (M.F.M.Y.)

Abstract: Frequency Response Analysis (FRA) technique has been recognized by worldwide utilities as a matured technology to assess the mechanical integrity of power transformers. While some industrial critical assets such as induction motors have the same construction principle as power transformers, the application of FRA technique to induction motors has not yet been fully explored. This paper presents analogical experimental studies for the application of FRA on power transformers and induction motors. For a consistent analogy, the FRA technique has been employed to detect short and open circuit turns in both appliances, which helps explore a wider scope of the FRA applications on rotating machines. In this regard, experimental FRA measurements are performed on an 11/0.415 kV, 500 kVA, three-phase distribution transformer and a 5.5 HP three-phase induction motor. Several short and open circuit faults are staged on the windings of both tested equipment and the FRA signature is recorded and compared with the reference signature at no fault. To quantify the impact of faults on the FRA signature, several statistical indicators are used and threshold limits for these indicators are proposed to automate the interpretation process. Results reveal a good correlation between the FRA signatures of induction motors and power transformers that attests to the feasibility of using FRA technique to detect various faults within large rotating machines.

Keywords: frequency response analysis; power transformer; induction motors; fault diagnosis; statistical indicators

Citation: Al-Ameri, S.M.; Alawady, A.A.; Abdul-Malek, Z.; Noorden, Z.A.; Yousof, M.F.M.; Salem, A.A.; Mosaad, M.I.; Abu-Siada, A. Frequency Response Analysis: An Enabling Technology to Detect Internal Faults within Critical Electric Assets. *Appl. Sci.* **2022**, *12*, 9201. https://doi.org/10.3390/app12189201

Academic Editor: Gaetano Zizzo

Received: 8 August 2022
Accepted: 13 September 2022
Published: 14 September 2022

1. Introduction

The power transformer is a critical link in electricity chains while the induction motor (IM) represents a critical asset for several industrial applications. While the reliability of power transformers is essential to assure the continuity of the power supply, IM reliability is crucial to avoid any unplanned interruption to the production line. Therefore, reliable diagnostic techniques must be adopted for both assets to detect faults at their early stages, and take remedial and timely action. A survey study reported that 40% of power transformer failures are due to the tap changer, while 30% are due to the main windings, as listed in Table 1 [1]. On the other hand, statistical studies conducted by the electric power research institute (EPRI) and the IEEE show that the bearings contribute the highest percentage of fault causes in rotating induction machines followed by faults within the stator windings as shown in Table 2 [2,3].

Table 1. Power transformer failure modes according to CIGRE international survey [1].

Failure Mode	Occurrence (%)
Tap changer	40
Main Windings	30
Bushing	14
Tank	6
Core	5
Auxiliary	5

Table 2. IM failures modes According to EPRI and IEEE surveys.

Failure Mode	Occurrence (%), EPRI	Occurrence (%), IEEE
Bearings	41	44
Stator winding	36	26
Rotor winding	9	8
Others	14	22

Several online and offline diagnostic techniques have been developed over the years to detect emerging faults within power transformers and IMs. Among these techniques, partial discharge (PD) measurement has been used to assess the insulation condition within transformers and IMs [4]. Other techniques to detect internal faults within transformers and IMs based on current-voltage signatures have been presented in the literatures [5,6].

Frequency response analysis (FRA) is an accepted commercial technology used to detect internal mechanical and electrical faults within power transformers [7]. As a matured technology for power transformers condition monitoring and fault diagnosis, several studies can be found in the literature to enhance its fault detection of which some are listed in Table 3. While FRA technology is not fully explored yet for IMs, a few relevant studies can be found in the literature, as summarized in Table 4.

Table 3. Research published on the application of FRA on power transformers.

Reference	Scope and Main Findings	Limitations
[8]	Application of support vector machine (SVM) for faults identification and quantification using FRA signatures. Results show the effectiveness of using SVM to analyze FRA signatures.	Lack of training data and inability to identify fault location.
[9]	Application of digital imaging to analyze FRA signature. Results reveal the ability of this method to detect several faults such as disc space variation and redial deformation.	Inability to identify the extent and location of the winding deformation.
[10]	Using transformer high-frequency equivalent circuits to understand FRA signatures. Results show that the physical meaning of circuit parameters can help understand the impact of several faults on the FRA signatures.	Lack of experimental verifications.
[11]	The simulation FRA results and the measurements FRA on actual windings were found very promising and encouraging to appraise the feasibility of the proposed measurement FRA method.	Only one experiment on one 3 MVA transformer unit was employed in the research.
[12]	FRA method and intelligence classifiers can be used to detect the transformer fault with a high level of accuracy.	Used parameters are based on estimation methods.
[13]	Estimation techniques in the study can be used for identifying and quantifying the FRA signatures in power transformers for fault analysis.	Simulation analysis was performed but was not verify practical measurement results.

Table 4. Research published on the application of the FRA on induction motors.

Reference	Scope and Main Findings	Limitations
[14]	Detecting broken bars in three-phase squirrel-cage IM using FRA. Results show a variation in the FRA signature within the frequency range 1 kHz to 300 kHz.	Only one fault was investigated, and no FRA interpretation methodology was presented.
[15]	Detecting short circuit faults within IMs. Findings show that turn−to−turn has a small effect on the motor FRA signature whereas a huge variation was observed for phase-to-phase short circuit fault.	Did not cover a variety of faults, and statistical indicators that are employed to interpret the results.
[16]	Detecting emerging winding faults. Reported results show that even a small percentage like 1% of winding defects can be detected by FRA.	Only turns fault at one phase is investigated and a few statistical indicators were used.
[17]	Detection of short circuit faults within IM.	Only Phase-to-phase fault is investigated with one assessment factor used to analyze the results.
[18]	Detecting winding faults within IM using FRA.	Interpretation of the result was based on personnel expertise.

FRA method displays a graphical signature of the electrical machine transfer function in a typical frequency range of 10 Hz to 2 MHz [19–21]. Changes occurring within the machine due to faults or insulation degradation are reflected on the FRA signature [22,23]. However, the main drawback of using FRA is that there is no widely approved standard or code to interpret the results, especially for rotating machines. Therefore, the FRA interpretation still depends on personal expertise. Some statistical indicators were proposed in the literature to quantify the comparison of FRA signatures [24,25].

A survey was conducted on the applicability of using various statistical indicators on FRA [26]. Among these indicators, correlation coefficient (CC), mean squared error (MSE), the absolute sum of logarithmic error (ASLE), root mean square error (RMSE), the absolute average difference (DABS), Covariance (COVAR), standard deviation (SD) and maximum-minimum ratio (MM) have shown high sensitivity to changes in the FRA responses. The drawback of using statistical indicators is that there are no approved benchmarks or threshold limits to identify and quantify various faults accurately.

From the above discussion, the problem can be stated as: FRA test has been successfully utilized for detecting mechanical deformations within power transformers, but the FRA application has not been widely extended to include other critical assets such as IMs. Furthermore, FRA interpretation for power transformer is still a challenging task due to the lack of standard interpretation codes. Hence, the main contribution of this paper can be summarized below:

- Presenting an analogical experimental study for the application of FRA on power transformers and IMs in order to understand and explore the wider application of the FRA technique on IMs.
- Employing several statistical indicators including CC, SD, ASLE, MSE, RMSE, DABS, COVAR and MM to calculate the variation between normal and faulty FRA signatures.
- Identifying threshold boundaries between normal and faulty cases or limits for the used statistical indicators to facilitate an easy and automated FRA interpretation process.

The paper is organized as follows. Section 1 presents a review on the application of the FRA method on transformers and IMs. In addition, the problem statement and study objective are stated in this section. Section 2 presents the FRA application for power transformers. In Section 3, the FRA application for IMs is presented. Section 4 presents the obtained results and analysis using several statistical indicators. A comparison of the FRA application on transformers and IMs is presented in Section 5. Finally, the main conclusions are drawn in Section 6.

2. FRA Applications on Power Transformers

2.1. Measurement Setup

FRA measurement in this paper is conducted on a 500 kVA, 11/0.415 kV, Dyn11 three-phase distribution transformer with a de-energized tap changer selector. The tap changer configuration is given in Table 5. The unit has been tanked off to conduct the FRA measurement with normal, short circuit (SC), and open circuit (OC) fault conditions. The un-tanked transformer windings are as shown in Figure 1 of which FRA measurement is carried out on phase-A of the high voltage (HV) with the commonly used end-to-end connection as shown in Figure 2. In this Figure, V_{in} is the input voltage with reference voltage V_{ref} at one terminal of one phase and V_{out} is the output voltage measured at the other terminal of the same phase while the low voltage (LV) winding is open. The FRA signature is the magnitude of the winding transfer function in dB (20 log10 V_{out}/V_{in}) measured in a frequency range of 10 Hz to 2 MHz [27]. Various SC turns are emulated using different tap changer positions while the normal winding condition is considered when the tap is at position 1 by connecting the terminals (4 and 5), as shown in Figure 3a. The minimum SC level is achieved at tap 2 when connecting tap terminals (3 and 5) while tap 1 is still in place, as described in Table 5. The SC at tap 3 is undertaken by connecting terminals (3 and 6), the SC at tap 4 is done by connecting terminals (2 and 6) and the SC at tap 5 is undertaken by connecting terminals (2 and 7) as presented in Table 5 and shown in Figure 3e. On the other hand, OC turns are performed by leaving tap 1 open at terminals (4 and 5).

Table 5. Tap changer configuration of the tested transformer.

Conditions	Description	Tap Connection	Position Showed in
1	Tap 1 Normal condition and remained connected in all cases	4-5	Figure 3a
2	Short at tap 2	5-3	Figure 3b
3	Short at tap 3	3-6	Figure 3c
4	Short at tap 4	6-2	Figure 3d
5	Short at tap 5	2-7	Figure 3e
6	Open circuit	No	Figure 3f

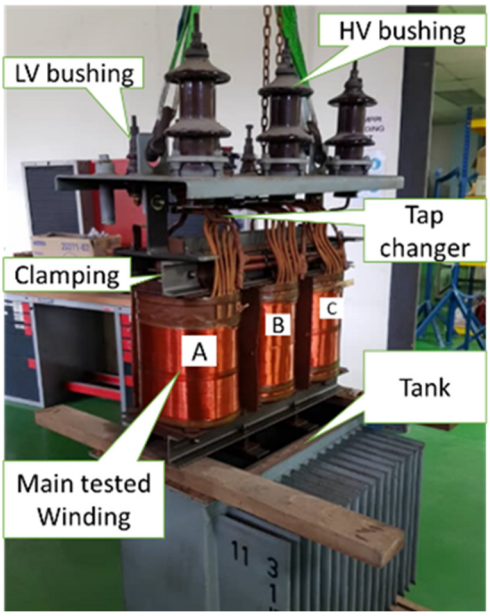

Figure 1. Tested distribution transformer windings.

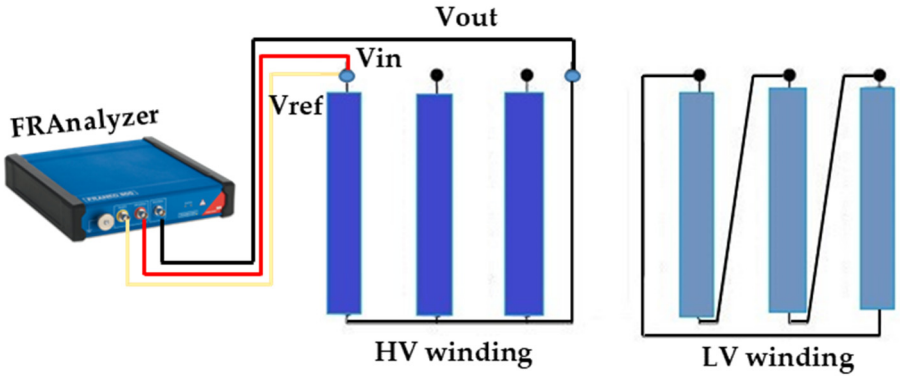

Figure 2. End-to-end winding FRA measurement connection.

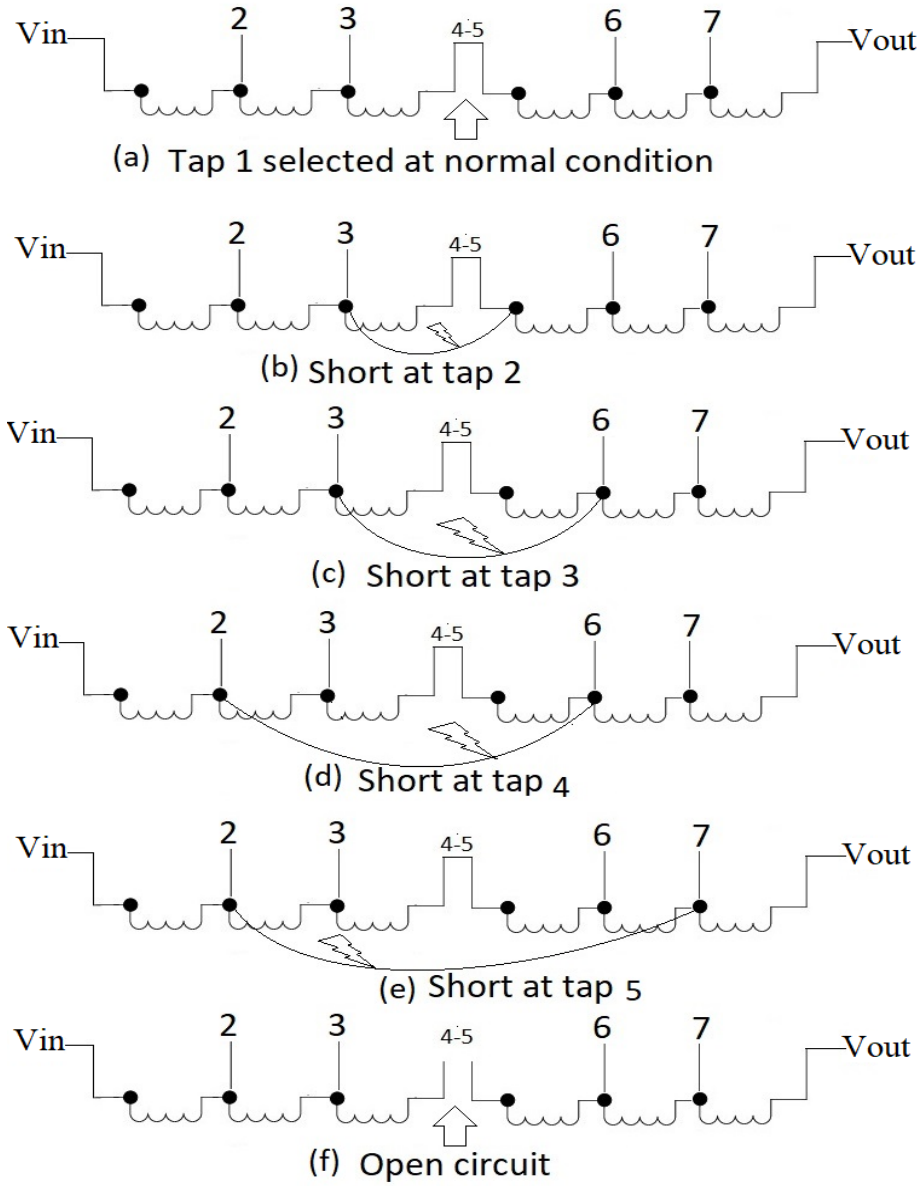

Figure 3. A schematic diagram for staging various SC and OC faults on the transformer winding.

A short circuit fault in a power transformer can occur when the condition of insulation between the adjacent turns of the conductor is degraded. In a power transformer, high voltage (HV) and low voltage (LV) windings are represented by series resistance Rs, series

capacitance Cs, and self-inductance Ls, respectively. The Gg and Cg are the ground conductance and capacitance which represent the insulation of the system. In the short circuit condition, the insulation system is degraded and the impedance (Z) of the winding changes. Short circuit fault is represented by reducing the operated amount of turns in the winding.

2.2. FRA Measurement Results

The measured FRA signatures for the SC and OC cases along with the signature for normal winding conditions are compared and shown in Figure 4. It can be seen from Figure 4a,b that the effect of SC turns on the transformer FRA signature is obvious in the frequency range 20 Hz to 10 kHz in which the magnitude of the winding transfer function is reduced, and the resonance point is shifted toward a higher frequency range compared to the normal signature. The variation in magnitude and resonance frequency increases with the increase of the SC level. On the other hand, Figure 4c shows a significant variation in the FRA signature obtained for OC turns in the low-frequency range. At the frequency range higher than 10 kHz, the FRA signature of the OC winding becomes similar to the winding normal signature. This may be attributed to the fact that, at such a high frequency and short OC gap, current can pass through the short gap based on the electromagnetic induction principle [28].

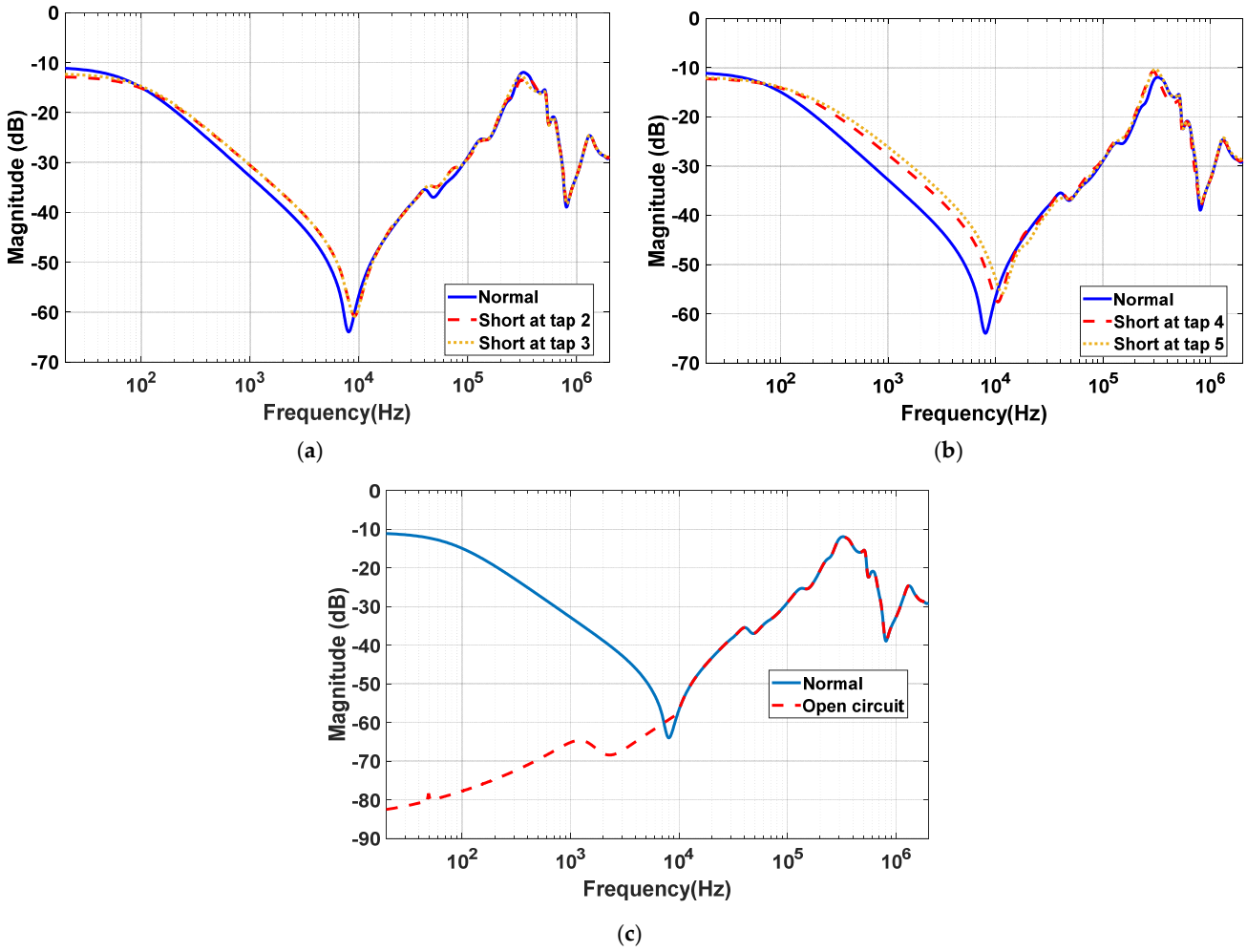

Figure 4. FRA measurement for the tested transformer winding at (**a**) Normal vs. SC at tap 2 and tap 3 (**b**) Normal vs SC at tap 4 and tap 5 (**c**) Normal vs. OC.

3. FRA Applications on Induction Motors

3.1. Measurement Setup

The FRA measurement is conducted on a three-phase 5.5 HP at 4 kW, 415 V, and 50 Hz IM as shown in the laboratory setup in Figure 5. Various SC faults are emulated on the stator winding including turn-to-turn SC, coil-to-coil SC, and phase-to-phase [29]. On the other hand, there is a ground fault which can be developed at phase, coil, turn and neutral points. In this study, the ground short circuit fault is artificially developed at four different points. A wire is connected to the ground from one turn, one full coil, or one full phase or the neutral point as shown in Figure 5 right inset. Figure 6 shows the mode of these faults along with the OC fault. Figure 7 shows the FRA measurement connection for star and delta stator windings. It is to be noted that in the case of star connection, the FRA analyzer can be connected between the two phases (U–V) or between one phase and the neutral point (U–N).

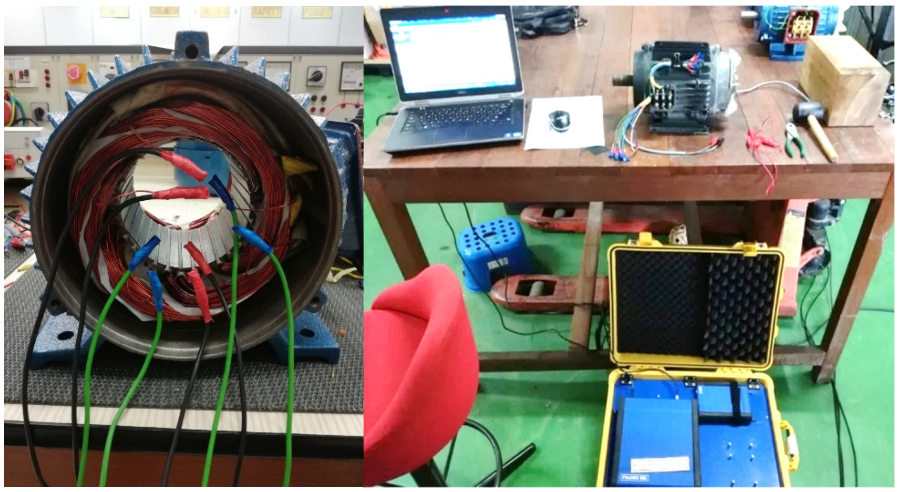

(**a**) (**b**)

Figure 5. Laboratory setup for IM FRA measurement and faults development (**a**) at fault development (**b**) during the FRA measurement.

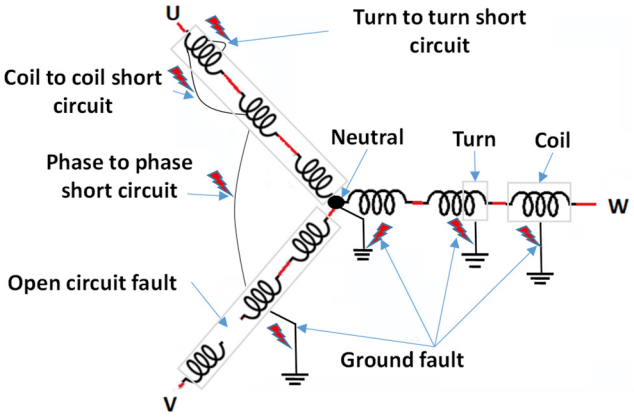

Figure 6. Schematic diagram for the emulated SC and OC faults on the stator windings.

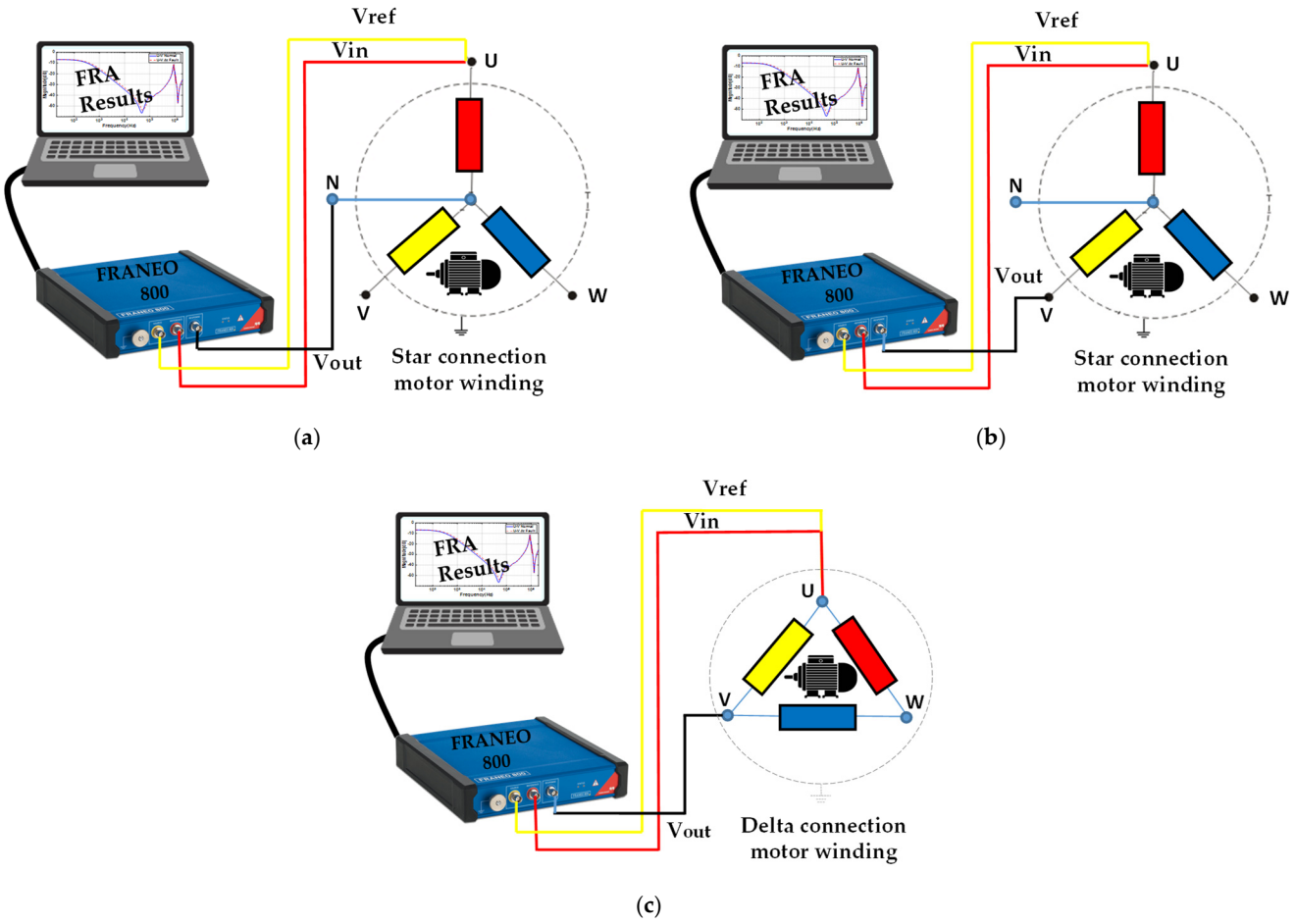

Figure 7. Schematic connection diagram for IM FRA measurement (**a**) U–N phase-to-neutral for star winding connection (**b**) U–V phase-to-phase for star winding connection (**c**) U–V phase for delta winding connection.

Like power transformers, the mechanisms of short circuit faults are due to insulation degradation. The number of operating turns reduces and winding conductor resistance increases.

3.2. FRA Measurement Results

FRA measurements have been conducted on the stator winding of the 5.5 HP IM while connected to star and delta configurations. The FRA trace of faulty cases is compared with the measured signature during normal conditions for the two winding configurations as shown in Figures 8 and 9, respectively. For star stator winding, Figure 8a shows a small decrease in the amplitude of the FRA signature due to turn-to-turn fault within the frequency range 200 Hz–100 kHz. The frequency response due to coil-to-coil SC shows more reduction in the amplitude when compared to the turn-to-turn SC fault. In contrast, the phase-to-phase SC fault shows an obvious variation in the magnitude and the resonance point at 50 kHz which is shifted to 100 kHz due to this fault. Figure 8b reveals no change in the FRA signature in the case of neutral-to-ground fault, a slight change in the magnitude due to coil-to-ground fault, and a change in the resonance frequencies due to turn-to-ground fault. As shown in Figure 8c, the OC fault has a significant impact on the FRA signature in the low-frequency range; the magnitude dropped from −10 dB (normal case) to −100 dB (OC case) at 10 Hz while in the high-frequency range over 100 kHz, the two FRA traces align perfectly. It is worth mentioning that these results are obtained based on the measurement

connection shown in Figure 7b. The FRA measurements for the connection topology shown in Figure 7a have a similar trend and are given in the Appendix A, Figure A1.

For the delta connection, Figure 9a,b show identical FRA patterns of SC faults to the star connection. Only the phase-to-phase SC fault produces a slight variation in the FRA signature as compared to the star connection. This is attributed to the outages of the two SC phases from the circuit in the case of star connection which is not the case for delta connection. It can be also seen that the FRA signature for phase-to-phase SC fault in delta stator winding is similar to that of turn-to-turn SC fault. Turn-to-ground fault FRA signature (Figure 9b) has a similar FRA pattern as the turn-to-ground in star connection. The coil-to-ground fault shows a little reduction in response magnitude within the frequency range of 50 k Hz to 100 kHz in the delta connection. The FRA pattern for OC fault (Figure 9c) shows a little variation that is different from the obtained pattern for star connection. The trace is shifted towards the low-frequency range with a slight in magnitude while it coincides with the normal trace at the high-frequency range reduction. This FRA's different pattern is due to the continuity of the supply current through the other two phases in the case of OC fault in one phase of the delta-connected winding.

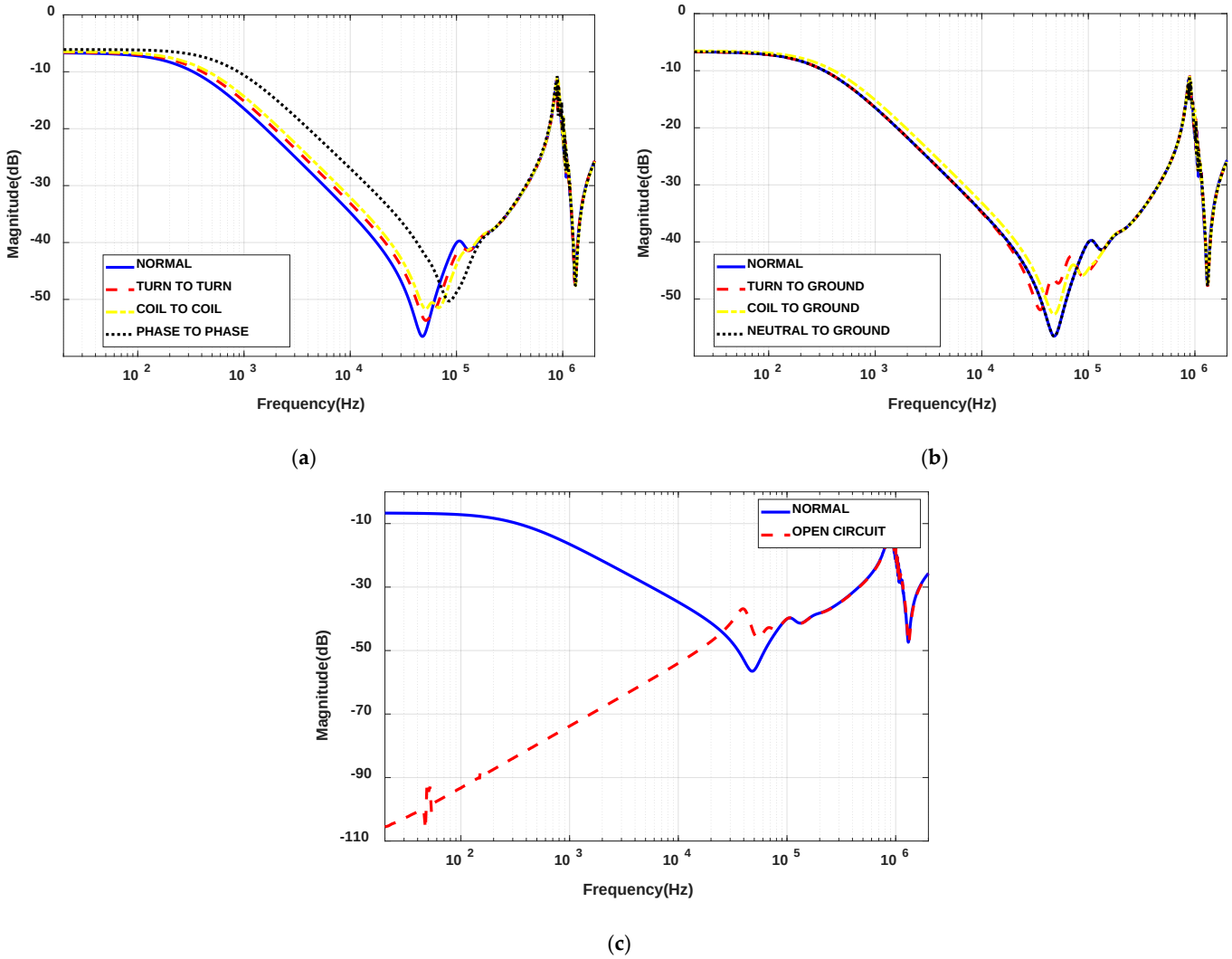

Figure 8. U–V FRA measured responses for the tested IM with stator star connection for (**a**) Normal vs turn−to−turn, coil−to−coil and phase−to−phase SC faults and (**b**) Normal vs turn−to−ground, coil−to−ground, and neutral−to−ground SC faults. (**c**) Normal vs. OC fault.

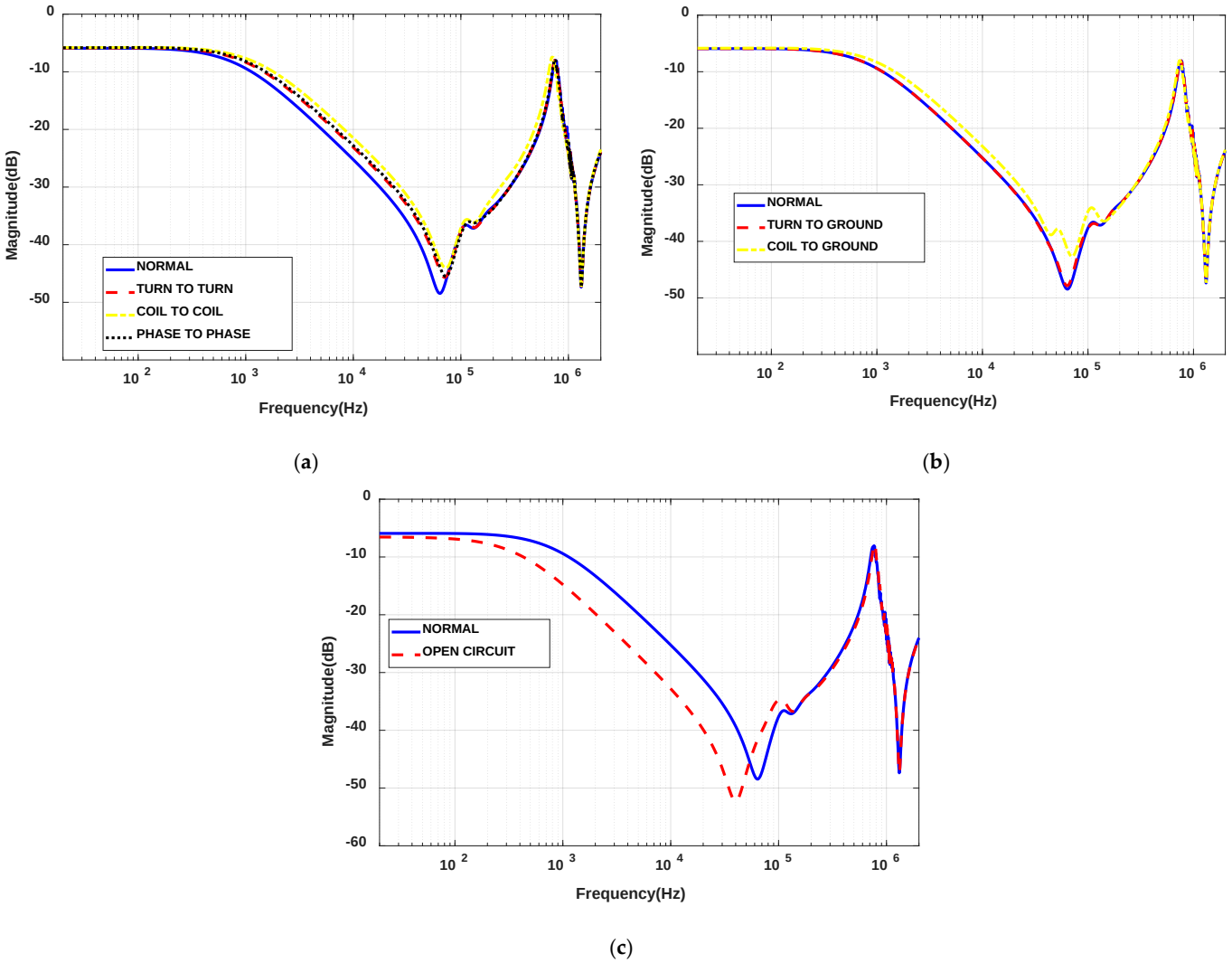

Figure 9. U–V FRA measured responses for the tested IM with stator delta connection for (**a**) Normal vs turn−to−turn, coil−to−coil, and phase−to−phase SC faults and (**b**) Normal vs turn−to−ground, and coil−to−ground SC faults, (**c**) Normal vs. OC fault.

FRA has been successfully used to test transformer mechanical condition. On the other hand, FRA test be extended to be used in rotating machines. Eventually, guidelines on the application of FRA for rotating machines such as IMs can be summarized as follows:

- End-to-end open circuit method can be adopted.
- FRA test should be performed in the manufacturer site and after installation to obtain the machine FRA signature.
- In case of no reference signature, users can use phase-to-phase comparison in order to detect any anomalies within the three measured signatures.
- Phase-to-phase measurement for delta windings can be conducted like the delta windings in power transformers.
- FRA measurement can be performed when there is any abnormal condition or severe fault within the machine.

4. FRA, Statistical Analysis

4.1. FRA Regions

To ease and automate the interpretation of FRA signatures, statistical indicators are used within multiple frequency ranges of the measured FRA signature. FRA regions for power transforms are standardized by the Cigre WG A2.26, IEC60076-18 Ed.1 and IEEE Std C57.149-2012 [19–21]. However, this division is not applicable for IM FRA signatures. Therefore, this paper proposes new regions for the IMs FRA signatures based on the significant changes and related effects of IM parameters. The low-frequency (LF) range is normally impacted by the resistive elements and magnetic flux, the middle frequency (MF) range is dominated by the inductive elements while the capacitive components affect the signature in the high-frequency (HF) range. At a very high-frequency range (VHF), the signature is mainly due to external wires and other parameters. The common FRA regions for the transformers and proposed regions for IMs are presented in Table 6.

Table 6. The common FRA regions limits for power transformers and the proposed regions for IMs.

FRA Regions	Transformers	IMs
LF	20 Hz–2 kHz	20 Hz–1 kHz
MF	2 kHz–20 kHz	1 kHz–80 kHz
HF	20 kHz–1 MHz	80 kHz–1 MHz
SHF	>1 MHz	>1 MHz

4.2. Statistical Indicators and Results

The statistical indicators can reveal the changes between two FRA data sets $X(i)$ and $Y(i)$ numerically. The CC has been recommended as a numerical indicator to measure the association of FRA signatures in previous studies [28]. The ASLE is one of the highly recommended statistical indicators to evaluate the absolute difference between two FRA data sets [28,30,31]. The use of SD has been proposed to calculate the variation among two FRA data sets. According to [26,32], the MSE, also known as sum, squared error (SSE), has a high sensitivity to changes in the FRA signatures. The RMSE is similar to the SD indicator. Compared with the MSE indicator, the RMSE is more appropriate to quantify the difference between two FRA traces. The absolute difference (DABS) metric is similar to ASLE, except that it does not perform logarithmic data conversion [32,33]. COVAR is used to measure the connection between two data sets while MM is very sensitive to the deviation of the response amplitude [32–34]. The reliance on one statistical indicator to diagnose FRA signatures is not satisfactory. For instance, the SD value is mainly controlled by the large data in the FRA set with less contribution from other data which affects its reliability. The CC cannot be used as a diagnostic indicator in some cases while the application of ASLE to diagnose FRA signatures still needs further research. Furthermore, the use of individual indicators does not reflect the actual fault level and an inconsistent trend of these indicators with the fault level has been reported in the literature [35,36]. The simultaneous use of several statistical parameters improves the reliability of the fault diagnosis process based on FRA measurement. Therefore, it is recommended to use a set of statistical parameters in a complementary way to increase confidence in the final decision. The selected statistical indicators in this paper are given by questions (1 to 8) in which X and Y represent the two FRA data sets to be compared and N is the total number of points within each set. The calculated values of these statistical indicators for normal and faulty conditions of the tested transformer and IM with a comprehensive comparison are presented in Tables 7–9.

The color coding refers to the threshold limits of the variation between the normal response and the fault responses. This method is used to evaluate and compare the indicators' ability for fault detection. The green color refers to the non-visible variation between the normal response and the fault response which can be detected by the indicator. The red color refers to the obvious variation between the normal and fault responses which can be noted in the indicator value. Thus, based on the notable indicator value, the variation can be detected and expressed by the red color.

The statistical indicators calculated in Tables 7–9 are analyzed in Table 10. The analysis was based on the indicator sensitivity to a fault (variation between the normal and fault responses), and the difference between its sensitivity to a fault in the power transformer and the IM.

$$CC_{(X,Y)} = \frac{\sum_{i=1}^{N} X(i) \times Y(i)}{\sqrt{\sum_{i=1}^{N}[X(i)]^2 \times \sum_{i=1}^{N}[Y(i)]^2}} \quad (1)$$

$$ASLE_{(X,Y)} = \frac{\sum_{i=1}^{N}|20log_{10}Y_i - 20log_{10}X_i|}{N} \quad (2)$$

$$SD_{(X,Y)} = \sqrt{\frac{\sum_{i=1}^{N}[Y(i) - X(i)]^2}{N-1}} \quad (3)$$

$$MSE = \frac{\sum_{i=1}^{N}(Y(i) - X(i))^2}{N} \quad (4)$$

$$RMSE = \sqrt{\frac{\sum_{i=1}^{N}(X(i) - Y(i))^2}{N}} \quad (5)$$

$$DABS = \frac{\sum_{i=1}^{N}|y(i) - x(i)|}{N} \quad (6)$$

$$COVAR(x,y) = \frac{1}{N}\sum_{i=1}^{N}(x(i) - \overline{x}(i)(y(i) - \overline{y}(i)) \quad (7)$$

$$MM = \frac{\sum_{i=1}^{N} min(Xi, Yi)}{\sum_{i=1}^{N} max(Xi, Yi)} \quad (8)$$

where:

x_i: is the data set from the first FRA measurement (signature of normal condition)
y_i: is the data set from the second FRA measurement (signature of fault condition)
N: the number of data set

Table 7. Statistical indicators for normal and faulty FRA signatures of the tested transformer.

Fault Type	Statistical Indicators											
	CC			ASLE			SD			MSE		
	LF	MF	HF	LF	MF	HF	LF	MF	HF	LF	MF	HF
SC at Tap 2	1.00	0.94	1.00	1.48	2.54	0.45	1.65	3.06	0.73	2.74	9.36	0.53
SC at Tap 3	1.00	0.94	1.00	1.54	2.54	0.44	1.65	3.05	0.70	2.91	9.32	0.50
SC at Tap 4	1.00	0.79	0.99	3.31	5.50	0.69	3.75	6.53	1.01	14.06	42.70	1.03
SC at Tap 5	0.99	0.65	1.00	4.21	7.35	0.66	4.83	8.45	0.95	23.40	71.46	0.90
Open circuit	0.28	0.43	1.00	49.54	8.95	0.35	51.04	10.97	0.51	260.52	120.55	0.26
Fault Type	**Statistical Indicators**											
	DABS			RMSE			COVAR			MM		
	LF	MF	HF	LF	MF	HF	LF	MF	HF	LF	MF	HF
SC at Tap 2	1.48	2.55	0.45	1.65	3.06	0.73	0.41	0.53	0.53	1.06	1.05	1.01
SC at Tap 3	1.54	2.54	0.45	1.70	3.05	0.70	0.42	0.53	0.54	1.06	1.05	1.01
SC at Tap 4	3.32	5.50	0.70	3.75	6.53	1.01	0.35	0.55	0.54	1.15	1.12	1.02
SC at Tap 5	4.22	7.35	0.66	4.83	8.45	0.95	0.32	0.56	0.62	1.21	1.17	1.02
Open circuit	49.55	8.95	0.36	51.04	10.97	0.51	0.49	0.49	0.51	3.04	1.19	1.01

Table 8. Statistical indicators for normal and faulty FRA signatures of the tested IM with star stator winding.

Fault Type	Statistical Indicators											
	CC			ASLE			SD			MSE		
	LF	MF	HF	LF	MF	HF	LF	MF	HF	LF	MF	HF
Turn to turn SC	1.00	1.00	0.99	0.79	1.59	0.94	0.91	1.60	1.59	0.84	2.55	2.54
Coil to coil SC	1.00	1.00	0.97	1.30	2.61	1.57	1.50	2.61	2.46	2.25	6.82	6.06
Turn to ground SC	1.00	1.00	0.96	0.00	0.13	1.61	0.01	0.22	2.88	0.00	0.05	8.28
Coil to ground SC	1.00	1.00	0.98	0.83	1.55	1.26	0.94	1.56	1.91	0.88	2.42	3.67
Neutral to ground SC	1.00	1.00	1.00	0.01	0.01	0.24	0.01	0.01	0.67	0.00	0.00	0.45
Phase to phase SC	0.99	1.00	0.83	3.41	7.58	3.58	4.01	7.59	5.85	7.07	7.61	7.19
Open circuit	−0.93	−1.00	0.91	71.59	26.59	2.23	28.97	28.97	4.62	5313.29	839.05	21.37
Fault Type	**Statistical Indicators**											
	DABS			RMSE			COVAR			MM		
	LF	MF	HF	LF	MF	HF	LF	MF	HF	LF	MF	HF
Turn to turn SC	0.79	1.59	0.94	0.91	1.60	1.59	0.07	0.41	0.05	1.07	1.05	1.03
Coil to coil SC	1.30	2.61	1.57	1.50	2.61	2.46	0.06	0.40	0.03	1.13	1.09	1.04
Turn to ground SC	0.00	0.13	1.61	0.01	0.22	2.88	0.08	0.42	0.08	1.00	1.00	1.05
Coil to ground SC	0.83	1.55	1.26	0.94	1.56	1.91	0.07	0.41	0.05	1.08	1.05	1.04
Neutral to ground SC	0.01	0.01	0.24	0.01	0.01	0.67	0.08	0.41	0.07	1.00	1.00	1.01
Phase to phase SC	3.41	7.58	3.58	4.01	7.59	5.85	0.03	0.38	0.02	1.41	1.32	1.11
Open circuit	71.59	26.59	2.23	72.89	28.97	4.62	−0.34	−0.44	0.15	7.14	1.85	1.07

Table 9. Statistical indicators for normal and faulty FRA signatures of the tested IM with delta stator winding.

Fault Type	Statistical Indicators											
	CC			ASLE			SD			MSE		
	LF	MF	HF	LF	MF	HF	LF	MF	HF	LF	MF	HF
Turn to turn SC	1.00	1.00	0.99	0.53	2.01	0.98	0.72	2.02	1.68	0.52	4.08	2.83
Coil to coil SC	1.00	1.00	0.97	0.89	3.54	2.18	1.21	3.56	2.86	1.46	7.65	8.17
Turn to ground SC	1.00	1.00	1.00	0.00	0.01	0.28	0.00	0.02	0.55	0.00	0.00	0.31
Coil to ground SC	1.00	1.00	0.98	0.56	1.96	1.40	0.74	1.96	2.27	0.55	3.84	5.16
Phase to phase SC	1.00	1.00	0.98	0.64	2.33	1.20	0.84	2.34	1.95	0.71	5.46	3.82
Open circuit	0.99	1.00	0.88	3.05	7.40	2.80	7.41	7.41	4.86	13.17	54.95	23.61
Fault Type	**Statistical Indicators**											
	DABS			RMSE			COVAR			MM		
	LF	MF	HF	LF	MF	HF	LF	MF	HF	LF	MF	HF
Turn to turn SC	0.53	2.01	0.98	0.72	2.02	1.68	0.01	0.33	0.00	1.07	1.10	1.03
Coil to coil SC	0.89	3.54	2.18	1.21	3.56	2.86	0.00	0.31	0.00	1.13	1.19	1.07
Turn to ground SC	0.00	0.01	0.28	0.00	0.02	0.55	0.01	0.35	0.00	1.00	1.00	1.01
Coil to ground SC	0.56	1.96	1.40	0.74	1.96	2.27	0.01	0.33	0.00	1.08	1.10	1.05
Phase to phase SC	0.64	2.33	1.20	0.84	2.34	1.95	0.01	0.33	0.00	1.09	1.12	1.04
Open circuit	3.05	7.40	2.80	3.63	7.41	4.86	0.02	0.38	0.00	1.40	1.34	1.09

Table 10. Statistical indicators sensitivity analysis and comparison of the obtained results for the power transformer and IM.

Indicator	Transformer Results (Table 7)	IM Results (Tables 8 and 9)
CC	CC is sensitive to SC faults in the MF region. The recorded values of CC due to SC at MF are <94. The CC also detects variations due to OC faults at LF and MF regions.	CC does not show the difference between normal and SC between turns, coil-to-coil, turn-to-ground, coil-to-ground and neutral-to-ground at LF and MF ranges. The values of CC are above 0.98 within these ranges. LF and MF regions recorded a variation with CC < 98 for OC fault in star-connected IM and the LF region for phase-to-phase SC fault. The CC detected more variation in the HF region for OC fault, phase-to-phase fault and little at the turn-to-ground, coil-to-coil and coil-to-ground and turn-to-turn.
ASLE	ASLE detects a variation in the responses of normal and faults conditions at LF and MF with a value >1.54.	Overall, ASLE detects the error between the normal, OC, and phase-to-phase faults at LF, MF and HF regions with a value > 1.5. The ASLE can reveal the effect of the coil-to-coil fault at MF and HF. ASLE can show the variation due to turn-to-turn and coil-to-ground at LF region LF and MF regions.
SD	The SD detects the variation between the normal and faulty signatures in LF and MF regions. The value of SD is >1.65. The SD does not detect any variation in the HF region where all values are <0.95.	The SD detects the error between the normal, OC, phase-to-phase and coil-to-coil faulty FRA signatures at LF, MF and HF regions with a value > 1.5. SD does not detect variations due to turn-to-ground fault. The minimum SD value that indicates fault for the turn-to-turn, coil-to-ground, and neutral-to-ground is 1.2 at LF and HF ranges.
MSE	MSE shows similar sensitivity to fault as ASLE and SD but with higher error values. According to MSE the faults caused a variation in LF and MF regions with a minimum error value of 2.74.	MSE shows a similar trend to SD based on the variation and ranges for the OC, phase-to-phase and coil-to-coil faults. However, the MSE shows higher values compared to ASLE. MSE indicates that turn-to-turn and coil-to-ground result in a variation in MF and HF regions with a minimum value of >1.5. The neutral-to-ground fault does not show variation. For the delta connection, the MSE does not show the variations in the FRA signature due to turn-to-ground.
DABS	DABS shows its sensitivity for faults in a transformer at LF and MF regions with a minimum value of 1.48.	DABS detects the variation over the entire FRA spectrum for OC fault and phase-to-phase fault for star connection. In the delta connection, DABS detects the variation at MF for phase-to-phase fault and the entire FRA range for OC fault. DABS shows the deviation at MF and HF regions for the coil-to-coil fault and MF range for the turn-to-turn and coil-to-ground. For turn-to-ground and neutral-to-ground faults, DABS does not show variation with all values being <1.09.
RMSE	RMSE is sensitive to faults in LF and MF regions and it has a minimum value of 1.65.	RMSE is sensitive to OC fault and phase-to-phase at LF and MF regions for star-connected IM with a minimum value of 2.2. RMSE detects the variation due to the coil-to-coil fault at LF, MF and HF regions with values >1.21. RMSE reveals values >1.21 for the coil-to-ground fault within the MF and HF regions and at the MF for the turn-to-turn fault. The values of RMSE are <1.21 for the turn-to-ground and neutral-to-ground faults.
COVAR	COVAR shows values <0.62 at HF region for tap 5 SC fault. COVAR values for all other faults are in the range (0.32–0.62).	COVAR values in LF and HF regions are less than 0.09. The values are notable at MF where the minimum COVAR value is above 0.20 in all cases. The COVAR shows a negative value for OC fault at LF and MF regions for star-connected IM.
MM	MM shows a notable variation at LF and MF for OC and SC faults at tap 4 and tap 5 with values >1.12. The other faults show similar values between (1.01–1.06).	MM can show some variation with values >1.11 for OC and phase-to-phase faults at LF and MF regions. For coil-to-coil SC fault, MM vales are >1.11 within the LF and MF regions for delta-connected IM. For turn-to-turn and coil-to-coil faults, MM shows the variation in the MF region. MM values for other faults are <1.09.

5. Comparison and Discussion

Based on the above experimental results, the FRA method can be effectively used to detect internal SC and OC faults within rotating machines in a similar way as power transformers. FRA can detect SC faults within power transformers with an observable variation at the MF range. FRA also detect the OC fault at LF and MF regions. These are the ranges where the winding resistance and inductance dominate the FRA trace. FRA can also

reveal the extent of SC faults, for instance, the used indicators reflected different values for SC at tap 1, lowest SC level and at tap 5, highest SC level.

FRA can also be employed to detect SC faults in IMs. The FRA measurements indicate that phase-to-phase fault has the largest variation between the normal and faulty responses over the entire FRA spectrum. Coil-to-coil and coil-to-ground faults results in noticeable variations in the FRA signature within the MF and HF regions. Turn-to-turn and turn-to-ground faults reveal variations in the MF region. The neutral-to-ground in a star-connected IM shows a small variation in the HF region. The OC fault has a different effect on the measured frequency response from star connection to delta connection. For star connection, the measured FRA shows a huge drop in the response at the LF and MF regions with no effect in the HF region. However, a relatively slight variation in the FRA signature can be noticed in the case of OC fault in a delta-connected IM in the LF and MF regions.

FRA detects the SC faults in the transformer within the frequency range of 100 Hz to 100 kHz while it detects SC faults in IM within the frequency range of 200 Hz to 500 kHz. FRA also detect the OC turns in the transformer with noticeable FRA variations in the frequency range of 20 Hz to 30 kHz, while this frequency range is 20 Hz to 100 kHz for star-connected IM and 20 Hz to 1 MHz for delta-connected IM.

While statistical indicators have been employed for fault identifications in power transformers, no specific limits were identified for most of these indicators to ease the identification and quantification process [37]. Based on the case studies in this paper, and by observing the analysis in Table 10, and the graphical FRA patterns of normal and faulty conditions, threshold values for the employed statistical indicators for power transformers and IMs are proposed, as listed in Table 11. The robustness of the proposed threshold limits can be attested through the for short-circuit and open-circuit case studies for transformer and IM.

Table 11. The proposed limits to determine the good condition of transformer and induction motors using FRA and statistical indicators.

Condition/Threshold Limit	CC	ASLE	SD	MSE	DABS	RMSE	COVAR	MM
Normal transformer	Above 94	<1.54	<1.65	<2.74	<1.48	<1.65	<0.53	<1.12
Normal IM	Above 0.98	<1.0	<1.2	<1.0	<1.0	<1.2	<0.2	<1.01

6. Conclusions

This paper presents an analogical experimental study to assess the feasibility of using FRA technology to detect internal faults within rotating machines. The paper is also aimed at providing a better understanding of the effect of faults within IMs on the FRA signature as compared to the effect of faults within power transformers. Similar to its application in power transformers, results show the ability of FRA to detect SC and OC faults within the stator winding of the IM. However, the measured FRA reveal dissimilar patterns in the two studied cases. In general, the IM results show that there is a minor variation between the faulty and normal FRA signatures at the MF and HF regions due to turn-to-turn, turn-to-ground, and coil-to-ground faults. It also shows average deviations due to coil-to-coil SC fault at the MF and HF regions. A significant variation within the entire frequency range can be noticed in the case of phase-to-phase SC and OC faults for the star-connected IM. Unlike the star stator winding, delta winding shows an average variation at the MF and HF regions due to phase-to-phase SC fault. To avoid misinterpretation of the FAR results, this paper recommends the adoption of several statistical indicators such as CC, SD, ASLE, MSE, RMSE, DABS, Covariance and MM to quantify the variation between the measured FRA signatures. From the results, a boundary between normal and faulty cases is provided or limits were proposed for each fault. Further research is essential to extend the application of FRA to detect other types of faults within different ratings of IMs to set more accurate threshold limits for the impact of each fault type on various statistical indicators. Also, the application of FRA to other assets such as power cables can be elaborated upon.

Author Contributions: Conceptualization, S.M.A.-A., M.F.M.Y. and A.A.-S.; methodology, S.M.A.-A., M.F.M.Y., Z.A.N. and A.A.A.; software, S.M.A.-A. and A.A.S.; validation, S.M.A.-A. and M.F.M.Y.; investigation, S.M.A.-A., M.F.M.Y. and Z.A.-M.; resources, S.M.A.-A. and M.F.M.Y.; writing—original draft preparation, S.M.A.-A. and M.F.M.Y.; writing review and editing, M.F.M.Y., Z.A.N., A.A.S., A.A.-S., M.I.M.; A.A.A. and Z.A.-M.; Project administration: M.F.M.Y., Z.A.N. and M.I.M. All authors have read and agreed to the published version of the manuscript.

Funding: This research was funded by the Ministry of Higher Education Malaysia under the Fundamental Research Grant Scheme Vot No (06E12, 4B482, 05G88, and 05G89). and The Islamic University, Najaf, Iraq.

Institutional Review Board Statement: Not applicable.

Informed Consent Statement: Informed consent was obtained from all subjects involved in the study.

Data Availability Statement: The data presented in this study are available in this article.

Acknowledgments: The authors gratefully acknowledge the Malaysia Ministry of Education and Universiti Teknologi Malaysia for funding this research with grant no 06E12, 4B482, 05G88, and 05G89. The authors would like to thank Mohd Aizam Talib from TNBR Malaysia for his assistance during the experiment. We would also like to thank all the subjects who volunteered to participate in this study.

Conflicts of Interest: The authors declare no conflict of interest.

Appendix A

The appendix presents the FRA measurement for the 5.5 HP IM phase-to-neutral (U–N) which could support the findings from the other U–V measurement. The used FRA measurement in the main content is for the phase-to-phase measurement which can show more details on the traces variation compare to phase measurement configuration.

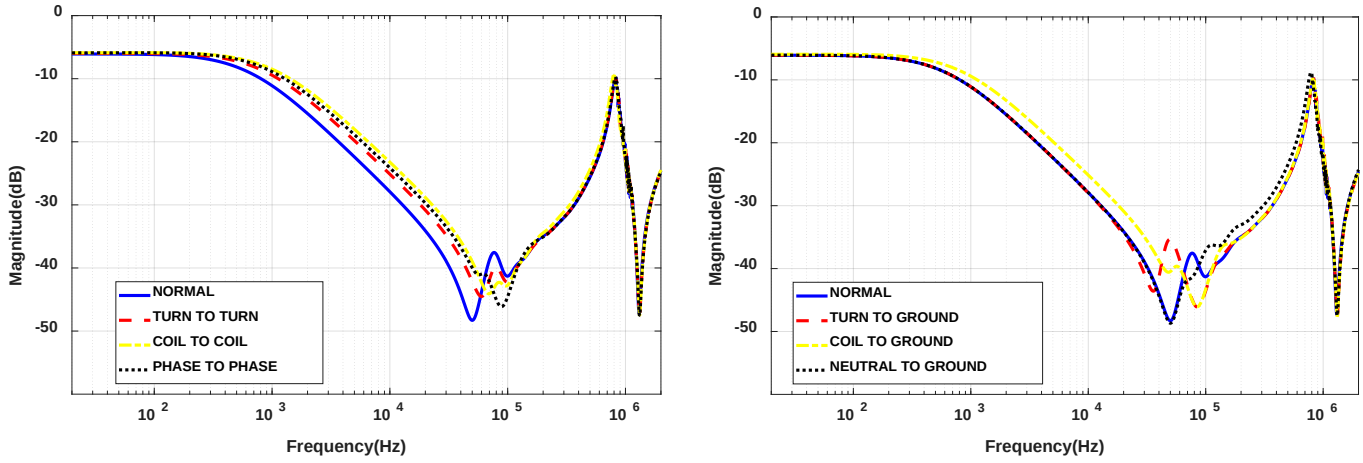

(**a**) (**b**)

Figure A1. U–N FRA measured responses for the tested IM with stator star connection for (**a**) Normal vs turn−to−turn, coil−to−coil, and phase−to−phase SC fault (**b**) Normal vs turn−to−ground, coil−to−ground, and neutral−to−ground SC faults.

References

1. Metwally, I. Failures, monitoring and new trends of power transformers. *IEEE Potentials* **2011**, *30*, 36–43. [CrossRef]
2. Motor Reliability Working Group. Report of Large Motor Reliability Survey of Industrial and Commercial Installations, Part I. *IEEE Trans. Ind. Appl.* **1985**, *IA-21*, 853–864. [CrossRef]
3. Cornell, P.F.E.P.; Owen, E.L.; Appiarius, J.C.; McCoy, R.M.; Albrecht, D.W.H. *Improved Motors for Utility Applications*; Final report; General Electric Co.: Schenectady, NY, USA, 1982. [CrossRef]
4. Florkowski, M.; Florkowska, B.; Zydron, P. Partial discharges in insulating systems of low voltage electric motors fed by power electronics—Twisted-pair samples evaluation. *Energies* **2019**, *12*, 768. [CrossRef]

5. Lee, S.B.; Shin, J.; Park, Y.; Kim, H.; Kim, J. Reliable Flux-Based Detection of Induction Motor Rotor Faults from the Fifth Rotor Rotational Frequency Sideband. *IEEE Trans. Ind. Electron.* **2021**, *68*, 7874–7883. [CrossRef]
6. Ma, G.; Liu, Y.; Li, Y.; Fan, X.; Xu, C.; Qin, W. Optical Frequency-Response Analysis for Power Transformer. *IEEE Trans. Power Deliv.* **2021**, *36*, 1562–1570. [CrossRef]
7. Zhao, Z.; Tang, C.; Yao, C.; Zhou, Q.; Xu, L.; Gui, Y. Improved Method to Obtain the Online Impulse Frequency Response Signature of a Power Transformer by Multi Scale Complex CWT. *IEEE Access* **2018**, *6*, 48934–48945. [CrossRef]
8. Liu, J.; Zhao, Z.; Tang, C.; Yao, C.; Li, C.; Islam, S. Classifying Transformer Winding Deformation Fault Types and Degrees Using FRA Based on Support Vector Machine. *IEEE Access* **2019**, *7*, 112494–112504. [CrossRef]
9. Zhao, Z.; Yao, C.; Tang, C.; Li, C.; Yan, F.; Islam, S. Diagnosing Transformer Winding Deformation Faults Based on the Analysis of Binary Image Obtained from FRA Signature. *IEEE Access* **2019**, *7*, 40463–40474. [CrossRef]
10. Mugarra, A.; Mayora, H.; Guerrero, J.M.; Platero, C.A. Frequency Response Analysis (FRA) Fault Diagram Assessment Method. *IEEE Trans. Ind. Appl.* **2022**, *58*, 336–344. [CrossRef]
11. Duvvury, V.S.B.C.; Pramanik, S. An Attempt to Identify the Faulty Phase in Three-Phase Transformer Windings Using an Advanced FRA Measurement Technique. *IEEE Trans. Power Deliv.* **2021**, *36*, 3162–3171. [CrossRef]
12. Bigdeli, M.; Siano, P.; Alhelou, H.H. Intelligent Classifiers in Distinguishing Transformer Faults Using Frequency Response Analysis. *IEEE Access* **2021**, *9*, 13981–13991. [CrossRef]
13. Abu-Siada, A.; Mosaad, M.I.; Kim, D.W.; El-Naggar, M.F. Estimating Power Transformer High frequency Model Parameters using Frequency Response Analysis. *IEEE Trans. Power Deliv.* **2020**, *35*, 1267–1277. [CrossRef]
14. Uhrig, S.; Ottl, F.; Hinterholzer, R.; Augeneder, N. Reliable Diagnostics on Rotating Machines using FRA. In Proceedings of the Proceedings of the 21st International Symposium on High Voltage Engineering, Budapest, Hungary, 26–30 August 2020. [CrossRef]
15. Yousof, M.F.M.; Alawady, A.A.; Al-Ameri, S.M.; Azis, N.; Illias, H.A. FRA Indicator Limit for Faulty Winding Assessment in Rotating Machine. In Proceedings of the 2021 IEEE International Conference on the Properties and Applications of Dielectric Materials (ICPADM), Johor Bahru, Malaysia, 12–14 July 2021; pp. 346–349. [CrossRef]
16. Vilhekar, T.G.; Ballal, M.S.; Umre, B.S. Application of Sweep Frequency Response Analysis for the detection of winding faults in induction motor. In Proceedings of the IECON 2016—42nd Annual Conference of the IEEE Industrial Electronics Society, Florence, Italy, 23–26 October 2016; pp. 1458–1463. [CrossRef]
17. Alawady, A.A.; Yousof, M.F.M.; Azis, N.; Talib, M.A. Phase to phase fault detection of 3-phase induction motor using FRA technique. *Int. J. Power Electron. Drive Syst.* **2020**, *11*, 1241–1248. [CrossRef]
18. Brandt, M.; Kascak, S. Failure identification of induction motor using SFRA method. In Proceedings of the 11th International Conference—2016 ELEKTRO, Strbske Pleso, Slovakia, 16–18 May 2016; pp. 269–272. [CrossRef]
19. Picher, P. Mechanical Condition Assessment of Transformer Windings Using Frequency Response Analysis (Fra). *Cigre Eval.* **2008**, *26*, 30–34.
20. *IEC 60076-18 Ed.1*; Power transformers—Part 18, 'Measurement of frequency response'. IEC: Geneva, Switzerland, 2012.
21. *IEEE Std C57.149-2012*; IEEE Guide for the Application and Interpretation of Frequency Response Analysis for Oil-Immersed Transformers IEEE Power and Energy Society. IEEE: Piscataway, NJ, USA, 2013; pp. 1–72. [CrossRef]
22. Cheng, B.; Wang, Z.; Crossley, P. Using Lumped Element Equivalent Network Model to Derive Analytical Equations for Interpretation of Transformer Frequency Responses. *IEEE Access* **2020**, *8*, 179486–179496. [CrossRef]
23. Nurmanova, V.; Bagheri, M.; Zollanvari, A.; Aliakhmet, K.; Akhmetov, Y.; Gharehpetian, G.B. A New Transformer FRA Measurement Technique to Reach Smart Interpretation for Inter-Disk Faults. *IEEE Trans. Power Deliv.* **2019**, *34*, 1508–1519. [CrossRef]
24. Samimi, M.H.; Tenbohlen, S.; Akmal, A.A.S.; Mohseni, H. Evaluation of numerical indices for the assessment of transformer frequency response. *IET Gener. Transm. Distrib.* **2017**, *11*, 218–227. [CrossRef]
25. Yang, Q.; Su, P.; Chen, Y. Comparison of Impulse Wave and Sweep Frequency Response Analysis Methods for Diagnosis of Transformer Winding Faults. *Energies* **2017**, *10*, 431. [CrossRef]
26. Sant'Ana, W.C.; Salomon, C.P.; Lambert-Torres, G.; da Silva, L.E.B.; Bonaldi, E.L.; Oliveira, L.E.D.L.D.; da Silva, J.G.B. A survey on statistical indexes applied on frequency response analysis of electric machinery and a trend based approach for more reliable results. *Electr. Power Syst. Res.* **2016**, *137*, 26–33. [CrossRef]
27. Kuniewski, M. FRA Diagnostics Measurement of Winding Deformation in Model Single-Phase Transformers Made with Silicon-Steel, Amorphous and Nanocrystalline Magnetic Cores. *Energies* **2020**, *13*, 2424. [CrossRef]
28. Kim, D.; Abu-Siada, A.; Sutinjo, A. State-of-the-Art Literature Review of WPT: Current Limitations and Solutions on IPT. *Electr. Power Syst. Res.* **2018**, *154*, 493–502. [CrossRef]
29. Ukil, A.; Chen, S.; Andenna, A. Detection of stator short circuit faults in three-phase induction motors using motor current zero crossing instants. *Electr. Power Syst. Res.* **2011**, *81*, 1036–1044. [CrossRef]
30. Ferreira, R.S.; Picher, P.; Ezzaidi, H.; Fofana, I. Frequency Response Analysis Interpretation Using Numerical Indices and Machine Learning: A Case Study Based on a Laboratory Model. *IEEE Access* **2021**, *9*, 67051–67063. [CrossRef]
31. Kim, J.W.; Park, B.; Jeong, S.C.; Kim, S.W.; Park, P. Fault Diagnosis of a Power Transformer Using an Improved Frequency-Response Analysis. *IEEE Trans. Power Deliv.* **2005**, *20*, 169–178. [CrossRef]

32. Badgujar, K.P.; Maoyafikuddin, M.; Kulkarni, S.V. Alternative statistical techniques for aiding SFRA diagnostics in transformers. *IET Gener. Transm. Distrib.* **2012**, *6*, 189–198. [CrossRef]
33. Secue, J.R.; Mombello, E. Sweep frequency response analysis (SFRA) for the assessment of winding displacements and deformation in power transformers. *Electr. Power Syst. Res.* **2008**, *78*, 1119–1128. [CrossRef]
34. Behjat, V.; Mahvi, M. Statistical approach for interpretation of power transformers frequency response analysis results. *IET Sci. Meas. Technol.* **2015**, *9*, 367–375. [CrossRef]
35. Banaszak, S.; Szoka, W. Analysis of Frequency Response measurement results with end-to-end/interwinding test setup correlation. *Arch. Electr. Eng.* **2018**, *67*, 51–64. [CrossRef]
36. Banaszak, S.; Szoka, W. Transformer Frequency Response Analysis with the Grouped Indices Method in End-to-End and Capacitive Inter-Winding Measurement Configurations. *IEEE Trans. Power Deliv.* **2020**, *35*, 571–579. [CrossRef]
37. Kennedy, G.; McGrail, A.; Lapworth, J. Transformer Sweep Frequency Response Analysis (SFRA), In *Energize*; Doble Engineering: Marlborough, MA, USA, 2007; pp. 28–33. Available online: https://www.ee.co.za/wp-content/uploads/legacy/Transformer_.pdf (accessed on 12 July 2022).